ISSN 2663-1563 Vol. 6, Issue 1: 26-41, DOI: 10.25236/AJAGE.2024.060105

Study of Thermal Energy Analysis of Composite Walls Based on Energy Plus Computational Simulation Method and Machine Learning

Xin Zuo[1], Die Liu[1], Qiao Zeng[1,*], Yunrui Gao[1], Yuhang Zhang[1]

[1]Chongqing College of Humanities, Science & Technology, Chongqing, 401520, China
[*]Corresponding author: 740556801@qq.com

Abstract: *The study confirms the impact of the thermal structure factor on heating energy usage through the interpretation of non-stationary heat transfer in composite walls using Green's function and the measurement of the magnitude of the thermal structure factor. The Energy Plus energy consumption simulation software was also employed to verify this effect. A proposed thermal structure factor, based on a theoretical analysis, reflects the order of material arrangement in each wall layer. This factor is specifically designed to improve the thermal characteristics and energy consumption analysis of the wall. Energy consumption simulation was then performed using energy analysis software. This was followed by field test research and analysis of heating energy consumption in energy efficient buildings. The beneficial research results provide guidance and implementation for current research and development in building energy efficiency.*

Keywords: *Building energy efficiency; Green's function; Thermal structure factor; Energy plus Energy consumption simulation; machine learning*

1. Introduction

This paper aims to advance the theoretical analysis of thermal characteristics and building energy consumption of composite walls from a novel perspective. Firstly, it is posited that the material and structural factors of the enclosure structure have an impact on the energy consumption of composite walls. The analytical solution for the unsteady heat conduction temperature field of composite walls is then presented, with reference to a pertinent example. In section two, we examine the unsteady heat conduction of a composite wall using Green function. We derive the expression for the Green function of the composite wall based on the current state of building energy conservation and apply this concept to explain the unsteady heat conduction of the wall. The third section analyses the structural features of the composite wall and the impact of material ordering on the composite wall's energy consumption. The fourth section introduces the concept of structural factors and investigates their effect on the energy consumption of composite walls. Section 5 analyses the thermal balance of the building envelope by creating an Energy Plus model and conducting simulations. To achieve accurate cooling load calculations, ASHRAE introduced the heat balance and radiation time series methods, and refined the calculation approach tied to the envelope structure's heat transfer process. Feng Zhong-zhong developed the cooling load coefficient method, utilising the transfer function technique and creating a suitable computer program for determining the building's annual hourly heating and cooling needs. Stephenson and Mitalas proposed the Z-transfer function method for calculating the unsteady heat transfer process of non-transparent envelopes. Quotes are clearly marked, and filler words have been avoided, while grammatical correctness and precise word choice are ensured. Differences in British and American spellings, vocabulary, and grammar have been observed and accounted for. Stephenson and Mitalas proposed the Z-transfer function method for calculating the unsteady heat transfer process of non-transparent envelopes. Technical terms are explained when first used, and a logical flow of information with causal connections between sentences is maintained. Our hypothesis has been proven through analysis and research. The language is clear, objective, and value-neutral, presented in a formal register with no biased or emotional language. The format adheres to style guides, with consistent citation and note formatting. This analysis identifies the factors that affect the thermal energy consumption of composite walls and indicates a direction for green building energy-saving walls. Addressing the task of quickly and accurately estimating the load of an enclosure structure, this paper analyses and condenses the primary impacting factors and subsequently formulates a correlation formula for the comprehensive

ISSN 2663-1563 Vol. 6, Issue 1: 26-41, DOI: 10.25236/AJAGE.2024.060105

heat transfer coefficient using the dimensionless analysis method. On this basis, Energy Plus calculates the simplified load calculation model for five representative cities, and verifies the accuracy of load calculations for several building sample groups. Subsequently, a novel evaluation approach is suggested for assessing thermal performance of building envelopes throughout the lifecycle. The limit value for the equivalent window-wall ratio in typical cities is calculated according to energy-saving regulations for residential buildings in various climate zones, and can aid in building design and energy efficiency. This serves as a reference for evaluation purposes. The load calculation is simplified to the product of the comprehensive heat transfer coefficient, building surface area, and temperature difference for load calculation. The calculated temperature difference for heating or cooling load is determined by subtracting the designed indoor temperature from the calculated outdoor temperature. A dimensionless correlation formula for the comprehensive heat transfer coefficient is derived based on dimensional theory. This coefficient is fundamental to the thermal assessment and comprehensive load calculation model of the envelope structure. Based on the comprehensive heat transfer coefficient of the building envelope, models calculating the cold and heat load indices and cumulative cold and heat load were developed for typical urban envelope structures found in Changchun, Beijing, Nanjing, Changsha and Nanning. Technical term abbreviations have been explained in their first use and the language used is clear, objective and formal. The text adheres to conventional academic structure and employs precise subject-specific vocabulary. The text already adheres to the principles - It provides an effective, rapid and accurate evaluation model and theoretical basis for the energy-efficient design of the enclosure structure, the load index estimation and energy consumption analysis of the enclosure structure in the air conditioning system, and the transformation of the enclosure structure to be more energy-efficient. Finally, this study demonstrates the practicality and rationality of the model, which provides an efficient, prompt, and precise evaluation model and theoretical foundation for designing energy-saving enclosure structures, optimizing building configuration, estimating load indexes, and analyzing energy consumption in air conditioning systems, as well as for energy-saving transformations of enclosure structures.

2. Materials and Processes

2.1 Non-stationary thermal conductivity of composite walls and the application of Green's function are the main points of concern

Three types of composite walls are distinguished based on insulation location: external insulation, internal insulation, and sandwich insulation. In this paper, the solution for the unsteady thermal conductivity of a single-layer wall under any class of boundary conditions will be derived. Additionally, the analytical solution for the temperature field distribution inside the wall when the temperature of the inner and outer surfaces of the wall varies with time will also be presented [1]. When the thickness of the wall is 6 to 10 times greater than its length and width, it can be considered as a one-dimensional heat transfer. If a single-layer uniform wall with a thickness of Lm and thermal conductivity of m^2/s has an initial temperature of $\phi(x)$ at time 0. It is assumed that the temperature of both sides of the wall will be $f_1(\tau)$ and $f_2(\tau)$, when time is greater than 0. If the thermal conductivity of the wall remains constant within a certain temperature range, the mathematical-physical equation of the wall can be determined.

$$\begin{cases} \frac{\partial T}{\partial \tau}=a\frac{\partial^2 T}{\partial x^2} \\ T(0,\tau)=f_1(\tau) \\ T(L,\tau)=f_2(\tau) \\ T(x,0)=\varphi(x) \end{cases} \tag{1}$$

In the equation, T denotes the temperature in degrees Celsius, L represents the wall thickness in metres, and represents the time in seconds. Furthermore, x represents the coordinate in the horizontal direction. To ensure that the equation satisfies the boundary conditions, the temperature function $T(x,\tau)$ is divided into two parts, $u(x,\tau)$ and $v(x,\tau)$.

$$\mathrm{T}(\mathrm{x},,\tau)=\mathrm{u}(\mathrm{x},,\tau)+\mathrm{v}(\mathrm{x},,\tau) \tag{2}$$

Which makes

$$\mathrm{v}(\mathrm{x},\tau)=\mathrm{f}_1(\tau)+\frac{\mathrm{x}}{\mathrm{L}}(\mathrm{f}_2(\tau)-\mathrm{f}_1(\tau)) \tag{3}$$

Then the function $u(x,\tau)$ conforms to the subsequent equation.

ISSN 2663-1563 Vol. 6, Issue 1: 26-41, DOI: 10.25236/AJAGE.2024.060105

$$\begin{cases} \frac{\partial u}{\partial \tau}=a\frac{\partial^2 u}{\partial x^2}+g(x,\tau) \\ u(0,\tau)=0 \\ u(L,\tau)=0 \\ u(x,0)=\varphi(x)-v(x,0) \end{cases} \tag{4}$$

Further, let u(x,τ) be defined as the sum of p(x,τ) and w(x,τ), where p(x,τ) and w(x,τ) satisfy equations (5) and (6) respectively.

$$\begin{cases} \frac{\partial p}{\partial \tau}=a\frac{\partial^2 p}{\partial x^2}+g(x,\tau) \\ p(0,\tau)=0 \\ p(L,\tau)=0 \\ p(x,0)=0 \end{cases} \tag{5}$$

$$\begin{cases} \frac{\partial w}{\partial \tau}=a\frac{\partial^2 w}{\partial x^2} \\ w(0,\tau)=0 \\ w(L,\tau)=0 \\ w(x,0)=u(x,0) \end{cases} \tag{6}$$

The non-singular equation in Equation 5 can be resolved by utilising the Fourier transform technique. Initially, Fourier series expansion is applied for both p(x,τ) and g(x,τ).

$$\mathrm{p}(\mathrm{x},\tau)=\sum_{\mathrm{n}=1}^{\infty}\mathrm{p_n}(\tau)\sin(\tfrac{\mathrm{n}\pi}{\mathrm{L}})\,\mathrm{x} \tag{7}$$

$$\mathrm{g}(\mathrm{x},\tau)=\sum_{\mathrm{n}=1}^{\infty}\mathrm{g_n}(\tau)\sin(\tfrac{\mathrm{n}\pi}{\mathrm{L}})\,\mathrm{x} \tag{8}$$

where the formula

$$\mathrm{g_n}(\tau)=\tfrac{2}{\mathrm{L}}\int_0^{\mathrm{L}}\mathrm{g}(\xi,\tau)\sin(\tfrac{\mathrm{n}\pi}{\mathrm{L}})\xi\mathrm{d}\xi \tag{9}$$

Then we can proceed.

$$g(x,\tau)=\sum_{n=1}^{\infty}\tfrac{2}{L}\int_0^{L}g(\xi,\tau)\,sin(\tfrac{n\pi}{L})\times sin(\tfrac{n\pi}{L})\xi d\xi \tag{10}$$

Substituting the above expansions into Equation 4 leads to:

$$\sum_{n=1}^{\infty}\sin(\tfrac{n\pi}{L})\times\left\{(\tfrac{n\pi}{L})^2 aP_n(\tau)+P_n(\tau)-g_n(\tau)\right\}=0 \tag{11}$$

If

$$(\tfrac{n\pi}{L})^2 a^2 P_n(\tau)+p_n'(\tau)-g_n(\tau)=0 \tag{12}$$

then there are

$$p_n'(\tau)=-(\tfrac{n\pi}{L})^2 a^2 P_n(\tau)+g_n(\tau) \tag{13}$$

have to

$$p_n(\tau)=\int_0^{\tau}\sum_{n=1}^{\infty}exp\left\{-(\tfrac{n\pi}{L})^2 a(\tau-\tau')g_n(\tau)d\tau'\right\} \tag{14}$$

$$\mathrm{p}(\mathrm{x},\tau)=\sum_{\mathrm{n}=1}^{\infty}\left[\int_0^{\tau}exp\left\{-(\tfrac{n\pi}{L})^2 a(\tau-\tau')g_n(\tau)d\tau'\right\}\right]\sin(\tfrac{\mathrm{n}\pi}{\mathrm{L}})\mathrm{x} \tag{15}$$

Above, the temperature field expression for the differential equation of unsteady thermal conductivity in a single-layer wall for any boundary conditions class is derived. Regarding the composite wall, it possesses an initial temperature ϕ(x) at the time of 0 based on the unsteady thermal conductivity of the single-layer wall. Assuming that the wall temperatures on both sides are f1 (τ), f2 (τ) respectively when the time exceeds 0, and the temperature conductivity of the layers of the composite wall remains constant within a specified temperature range without any contact thermal resistance between the layers [2].

The temperature distribution of a composite flat wall remains continuous. If any layer can be assumed as homogeneous, the differential equation of thermal conductivity applies.

$$\begin{cases} \frac{\partial T_i}{\partial \tau}=a_i\frac{\partial^2 T_i}{\partial x^2}+g(x,\tau)\quad (i=1,2,\cdots,M) \\ T_i(0,\tau)=f_1(\tau) \\ T_M(l_m,\tau)=f_2(\tau) \\ T_i(x,0)=\varphi_i(x) \end{cases} \tag{16}$$

ISSN 2663-1563 Vol. 6, Issue 1: 26-41, DOI: 10.25236/AJAGE.2024.060105

Where i represents the sequential number of each layer of the composite wall, with Li being the thickness, li denotes the x-coordinate, and Ti indicating the room temperature in degrees Celsius. Each layer of the composite wall has its own differential equation of thermal conductivity. When the interior wall has the same thickness, the thermal conductivity of the wall material is proportional to the Green's function value, which also conforms with the thermal conductivity theory of the wall. When the thermal conductivity is higher, the instantaneous point heat source has a greater impact on the wall, which increases the value of the Green's function and subsequently raises the temperature of the wall. Conversely, lower thermal conductivity weakens the effect of the point heat source on the wall, resulting in a smaller Green's function value and a lower wall temperature.

2.2 The Impact of Composite Wall Material Sequencing on Energy Consumption

According to the location of the insulation layer of different composite insulation wall is mainly divided into: external insulation, internal insulation and sandwich insulation. External insulation composite walls are generally cast with bonding mortar or directly with special fasteners, the insulation material is attached to the outside wall of the building, the outside is smeared with anti-cracking mortar, and then pressed into the mesh glass fibre so that it forms the outer protective layer, and finally made into a decorative surface [3]. Internal insulation composite walls are produced by adding insulation material to the inside of a building's exterior wall structure. The sandwich insulation composite wall enables direct molding of the insulation material with the wall using a one-time pouring technology. The insulation panels are placed inside the building formwork of the concrete frame, while concrete is poured on the exterior side of the wall. This process results in a composite wall [4].

The temperature difference between the air inside and outside the wall on both sides is 1 degree Celsius, and the heat transfer through the unit area of the wall in W/(m^2.K) per unit time is expressed in K. The heat transfer capacity of the air on both sides of the wall when passing through the wall is from indoor → wall → outdoor [5]. Another parameter corresponding to the total heat transfer coefficient K value of this heat transfer process is the heat transfer resistance of the enclosure R T. Its mathematical description and relationship are as follows:

$$K = \frac{Q}{A(T_i - T_e)} = \frac{q}{T_i - T_e} \tag{17}$$

$$R_T = \frac{T_i - T_e}{q} = \frac{1}{K} \tag{18}$$

$$R_T = R_i + \sum_{m=1}^{M} R_m + R_e \tag{19}$$

The heat transfer coefficient of the wall, represented by K, is measured in units of W/(m^2.K);

R_T — The total thermal resistance of heat transfer through the wall is measured in m^2·K/W;

Q — the heat transfer through the wall, W;

T_i — ambient room temperature, K;

T_e — outdoor ambient temperature, K;

A — radiant area of heat through the wall, m^2;

q — Q heat flow density W / m^2 ;

R_i — thermal resistance of heat transfer between indoor air and inner wall, m^2·K/W.

R_e — thermal resistance of heat transfer between the outdoor air and the inner wall, m^2·K/W.

R_m— thermal resistance of thermal conductivity of the layers of the wall,m^2·K/W.

M — number of wall layers

The total heat capacity of the composite wall can be calculated according to the following equation (20).

$$C_T = \frac{\sum_{m=1}^{M} \rho_m c_m L_m}{\sum_{m=1}^{M} L_m} \tag{20}$$

where C_T — the total heat capacity of the composite wall in the direction of the unit cross-section, kJ/ K;

L_m — the thickness of the layers of material of the composite wall, m;

ISSN 2663-1563 Vol. 6, Issue 1: 26-41, DOI: 10.25236/AJAGE.2024.060105

ρ_m— density of the layers of the composite wall material, kg/m^3;

c_m — specific heat of the layers of the composite wall material, kJ/kg.k

The building envelope wall is frequently in an unstable state of heat transfer. Generally, the thermal inertia index comprises the product of the thermal resistance and heat storage coefficient of each material layer of the wall used to estimate the thermal performance [6,7]. The following formula calculates D_T for the thermal inertia index for composite walls in the current code.

$$D_T = \sum_{m=1}^{M} D_m \tag{21}$$

$$D_m = R_m \cdot S_m \tag{22}$$

where D — the thermal inertia index of the wall.

D_m — the thermal inertia index of the material of each layer of the wall.

R_m — thermal resistance of the material layer, m^2 ·K/W.

S_m — heat storage coefficient of the material, W / m^2 ·K

The heat transfer coefficient, heat capacity and thermal inertia index for the wall can be calculated by adding the formulas that accumulate the parameters of each material layer present, under the condition of a steady-state heat transfer. This calculation is not dependent on the layer arrangement order but rather on the thickness of every material layer, its corresponding heat capacity, thermal conductivity, convective heat transfer coefficient of the inner and outer surfaces, and air [8].

The weather forecast indicated a high of 9.5℃ and a low of -13.5℃, resulting in an average daily temperature difference of 10.13℃. Temperature readings from the hospital's temperature and humidity recorder revealed a maximum temperature of 5.9℃ and a minimum temperature of -19.4℃, resulting in a daily average temperature difference of 13.6℃. Please refer to Figure 1 for specific regional variations in temperature.

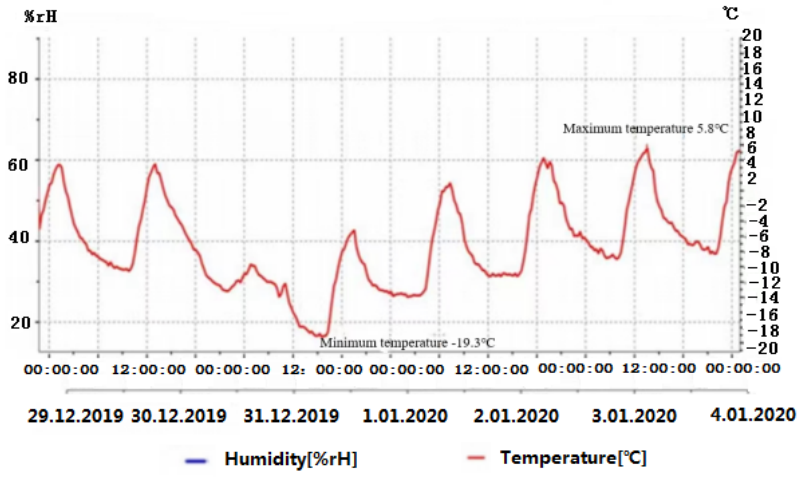

Figure 1: Local temperature change during the test

Figure 2 illustrates the variation in building temperature and humidity under external insulation walls, internal insulation walls, and sandwich insulation walls, respectively.

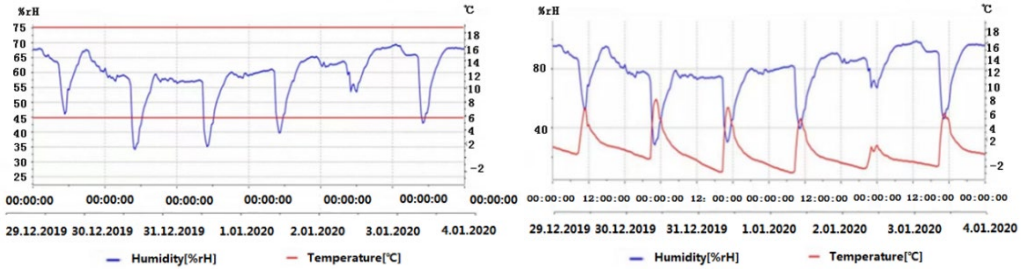

(a) *(b)*

ISSN 2663-1563 Vol. 6, Issue 1: 26-41, DOI: 10.25236/AJAGE.2024.060105

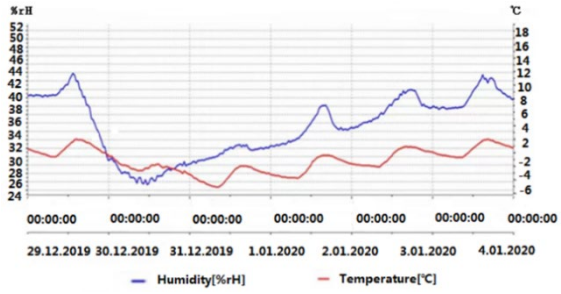

(c)

Figure 2: Temperature and humidity change curves under different insulation walls: (a) external insulation wall, (b) inner insulation wall, (c) sandwich insulation wall.

3. Results

From the above analysis, it is evident that the inhibition of temperature fluctuations in composite walls composed of layers with the same materials but arranged differently has a significant impact on indoor temperature, humidity, and envelope structure.

The building envelope plays a crucial role in controlling the amount of energy consumed by the building [9]. The efficiency of the envelope's sealing and thermal insulation has a direct impact on the size of a building's energy consumption. As the envelope's different components vary in area and physical properties, there are discrepancies in their energy consumption. Energy use is proportionate to the exterior walls, exterior windows, door and window gaps, and the house as demonstrated in Figure 3.

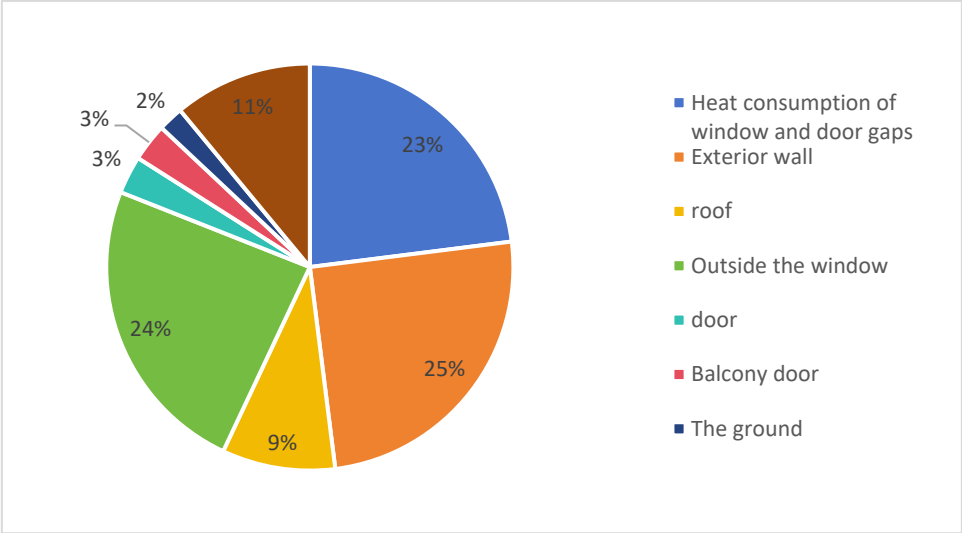

Figure 3: Energy consumption of each component of building envelope

3.1 Analysis of the influence of thermal structure factor on the thermal energy consumption of composite walls

Under non-steady state heat transfer conditions, the wall restrains the change in ambient temperature on both sides when the microclimate of either the indoor or outdoor environment changes. Its inhibitory capability is primarily reliant on the density and order of arrangement of the wall layers [10]. In the temperature field of a single-layer homogeneous wall under steady-state conditions, assuming that the wall thickness of the studied structure is L, it is placed in both an indoor and outdoor environment with Ti and Te. The wall material is singular and possesses uniform thermal properties, such as thermal conductivity λ. Assuming both sides of the wall have constant convective heat transfer thermal resistance (Ri and Re, respectively) and that the specific heat and density of the wall remain constant, and Ti and Te remain unchanged over time, a constant heat flow will occur through the wall's surface. The deformation of Equation 18 produces these results.

ISSN 2663-1563 Vol. 6, Issue 1: 26-41, DOI: 10.25236/AJAGE.2024.060105

$$q = \frac{T_i - T_e}{R_T} \tag{23}$$

$$R_T = R_i + R_e + R \tag{24}$$

$$R = L/\lambda \tag{25}$$

where L — the thickness of a single layer of wall, m;

λ — thermal conductivity of a single layer homogeneous wall, W/ m.K;

Assuming θ represents the temperature without influencing factors during steady-state heat transfer, the factorless temperature field.

θ(x) can be expressed as:

$$\theta_{(x)} = \frac{T(x)-T_i}{T_e-T_i} = \frac{R_{i-x}}{R_T}, \quad 1-\theta(x) = \frac{R_{x-e}}{R_T} \tag{26}$$

where R_{i-x} — heat transfer thermal resistance from the inside of a single layer wall to point x, m^2.K/W.

R_{x-e}— heat transfer thermal resistance from point x within a single layer wall to the outside, m^2.K/W.

Then the temperature field of the one-dimensional steady-state single-layer homogeneous wall is

$$T(x) = \theta(x)(T_e - T_i) + T_i \tag{27}$$

In the temperature field of a multi-layer homogeneous wall, referring to a composite wall of M-layer material as depicted in Figure 1, where each layer of the composite wall is numbered sequentially as m, and the thickness denoted by Lm, and x-coordinate denoted by lm, the relationship lm - lm-1 = Lm holds. Given steady-state conditions, the temperature field distribution at any point x within the composite wall can be determined.

$$\begin{cases} T(x) = T_i = \frac{T_i - T_e}{R_T} \cdot \left(\frac{l_1}{\lambda_1} + R_i\right), x \in (0, l_1) \\ T(x) = T_{m-1}(x) + \frac{T_i - T_e}{R_T} \cdot \left(\frac{l_x - l_{m-1}}{\lambda_m} + R_i\right), x \in (l_{m-1}, l_m) \end{cases} \tag{28}$$

Denote by i the temperature field of each layer of the composite wall without factorization, then

$$T(x) = \theta(x)(T_e - T_i) + T_i \tag{29}$$

$$\theta(x) = \frac{T(x)-T_i}{T_e-T_i} = \frac{R_{i-x}}{R_T} \tag{30}$$

where R_{i-x} and R_{x-e} can be derived from the following integral equation.

$$R_{i-x} = R_i + \int_0^x \frac{dx'}{\lambda(x')}, R_{x-e} = \int_x^{l_M} \frac{dx'}{\lambda(x')} + R_e \tag{31}$$

$$R_T = R_{i-x} + R_{x-e} = R_i + \int_0^x \frac{dx'}{\lambda(x')} + \int_x^{l_M} \frac{dx'}{\lambda(x')} + R_e = R_i + \sum_{m=1}^{M} R_m + R_e \tag{32}$$

Assuming that the ambient temperature changes, and at τ = τ1, Ti1 and Te1 are the temperatures on both sides, and at τ = τ2, these temperatures change to Ti2 and Te2 and remain constant. Within the time period (τ1 ,τ1), if enough time has elapsed and the initial and final states represent two distinct steady-state states, the temperature field in each part of the wall changes, but the wall's interior temperature field remains unchanged. The temperature at any point x of the wall changes during these two state changes.

$$\Delta T(x) = \theta(x)\Delta T_e + (1-\theta(x))\Delta T_i \tag{33}$$

It can be seen that due to the change of ambient temperature on both sides, the size of the temperature change at any point of the wall depends on.

The temperature profile of the wall is determined by the thermal resistance of the wall and the magnitude of the temperature difference between the environments on either side [11]. During a period of temperature change on both sides, a single layer homogeneous flat plate wall experiences heat flow on the indoor side due to the ambient temperature changes on both the indoor and outdoor sides. This results in corresponding changes in the heat flow expressions on both sides of the wall, as shown in equations (34) and (35). Technical terms will be explained when first introduced. Common academic sections will be included and consistent citation and footnote styles will be utilized. Language will remain formal, clear, objective and value-neutral. Biases will be avoided and grammatical correctness will be ensured to improve academic writing quality. During the period t2-t1, the heat at the wall can be split

ISSN 2663-1563 Vol. 6, Issue 1: 26-41, DOI: 10.25236/AJAGE.2024.060105

into two parts. The first component is the heat flow caused by the temperature difference between the two sides over time. The other component is the extra heat due to the change in ambient temperature on both sides [12]. It is plausible to consider that the accumulation of heat transferred over time, as a result of the temperature disparity between both sides, is almost equivalent over a considerably long period at both walls.

$$Q_i(t) = \frac{\Delta\tau}{R_T}[T_{im} - T_{em}] + C\varphi_{ii}\Delta T_i + C\varphi_{ie}\Delta T_e \quad (34)$$

$$Q_e(t) = \frac{\Delta\tau}{R_T}[T_{im} - T_{em}] + C\varphi_{ie}\Delta T_i + C\varphi_{ee}\Delta T_e \quad (35)$$

Where: Q_e (t) — heat flow at the outer wall of the composite wall, kJ/ m^2;

Q_i (t) — heat flow at the inner wall of the composite wall, kJ/ m^2 ;

R_T — thermal resistance of the composite wall m^2. K /W;

C — total heat capacity of the composite wall in the direction of the unit cross-section, kJ/ m2 /K;

T_{im} — average of the air temperature on the interior side of the composite wall, K;

T_{em} — average of the air temperature on the interior side of the composite wall, K;

$C\varphi_{ee}\Delta T_e$ — heat transferred to the outside wall of the composite wall due to the change of the outside ambient temperature, kJ/ m^2;

$C\varphi_{ii}\Delta T_i$ — heat transferred to the inside wall of the composite wall due to the change of the inside ambient temperature, kJ/ m^2;

$C\varphi_{ie}\Delta T_i$ — heat transferred to the outer wall of the composite wall due to the change of the outer ambient temperature, kJ/ m^2;

$C\varphi_{ie}\Delta T_e$ — heat transferred to the outer wall of the composite wall due to the change of the inner ambient temperature, kJ/ m^2.

φ_{ee} — the outer factor of the composite wall structure, the heat correction factor of the heat stored inside the composite wall through the outer wall of the composite wall due to the change of the outer ambient temperature;

φ_{ii} — the inner factor of the composite wall structure, the heat correction factor of the heat stored inside the composite wall through the inner wall of the composite wall due to the change of the inner ambient temperature the heat correction coefficient of the heat stored in the composite wall through the inner side wall of the composite wall due to the change of the inner ambient temperature;

φ_{ie} — the factor in the composite wall structure, the heat correction coefficient of the heat stored in the composite wall through the outer side wall of the composite wall due to the change of the inner ambient temperature;

Table 1: The thermal property of different material of exterior wall

Name of Material	λ w/m.K	ρ kg/m^3	C_p kj/kg.K
Lime mortar surface	0.83	1650	1.12
Polystyrene plate	0.046	32	1.42
Clay solid brick walls	0.86	1850	1.22
Cement mortar surface	0.98	1860	1.22
Cast-in-place reinforced concrete	1.82	2550	0.98

The thermal structure factor of multi-layer composite walls is determined by the arrangement order of thermal resistance and heat capacity for the materials within each layer of the wall. Analysis was conducted on two groups of four energy-efficient composite insulation walls, each with the same thermal resistance and heat capacity but different material arrangement orders. Expanded polystyrene foam, abbreviated as EPS, is the main component of the EPS external insulation system. This system is composed of adhesive, EPS boards, alkali-resistant glass fiber mesh cloth, and plastering slurry leveled into a new wall construction system that provides both insulation and decorative functions. EPS external insulation systems are suitable for a variety of external wall insulation compounds in new and old buildings facing energy-saving challenges.

ISSN 2663-1563 Vol. 6, Issue 1: 26-41, DOI: 10.25236/AJAGE.2024.060105

Table 1 illustrates the thermal parameters of the materials used in each layer of the combined wall.

The structure of the composite insulated wall is shown in Table 2.

Table 2: Eight construction of outer insulation- exterior wall

Name of Composite wall		The first layer	The second layer	The third layer	The fourth floor	The fifth floor	Total thickness
EPS external insulation wall	Name of Material	Lime mortar surface	Clay solid brick walls	Polystyrene plate	Cement mortar surface	———	0.42
	thickness	0.12	0.28	0.12	0.12		
EPS internal insulation wall	Name of Material	Lime mortar surface	Polystyrene plate	Clay solid brick walls	Cement mortar surface	———	0.42
	thickness	0.12	0.18	0.28	0.13		
EPS central wall	Name of Material	Lime mortar surface	Clay solid brick walls	Polystyrene plate	Clay solid brick walls	Cement mortar surface	0.42
	thickness	0.12	0.16	0.18	0.14	0.02	
EPS central wall1	Name of Material	Lime mortar surface	Polystyrene plate	Solid wall of clay	Polystyrene plate	Cement mortar surface	0.42
	thickness	0.12	0.15	0.24	0.15	0.02	
Cast-in-place reinforced concrete polystyrene board external insulation wall	Name of Material	Lime mortar surface	Cast-in-place reinforced concrete	Polystyrene plate	Cement mortar surface	———	0.48
	thickness	0.12	0.32	0.13	0.12		
Cast-in-place reinforced concrete polystyrene board internal insulation wall	Name of Material	Lime mortar surface	Polystyrene plate	Cast-in-place reinforced concrete	Cement mortar surface	———	0.44
	thickness	0.12	0.14	0.36	0.12		
Cast-in-place reinforced concrete polystyrene board central wall	Name of Material	Lime mortar surface	Cast-in-place reinforced concrete	Polystyrene plate	Cast-in-place reinforced concrete	Cement mortar surface	0.44
	thickness	0.12	0.16	0.18	0.18	0.12	
Cast-in-place reinforced concrete polystyrene board central wall1	Name of Material	Lime mortar surface	Polystyrene plate	Cast-in-place reinforced concrete	Polystyrene plate	Cement mortar surface	0.44
	thickness	0.12	0.15	0.28	0.15	0.12	

Convective heat transfer thermal resistance on both sides of the composite wallR_i =0.12 m^2 ·K/W, vs.R_e =0.05m^2·K/W. Eight different composite insulated walls with thermal structure factorsφ_{ii} , φ_{ee} , andφ_{ie} According to equations (31), (34) and (35), the data of their thermal structure factors can be obtained as in Table 3.

The impact of composite walls on changes to ambient temperature is influenced by the heat capacity

ISSN 2663-1563 Vol. 6, Issue 1: 26-41, DOI: 10.25236/AJAGE.2024.060105

of the material used in the building envelope. This capacity increases with greater material density, specific heat and thickness. It is important to note that the specific heat and thickness of various types of building walls do not differ significantly, whereas the density of different materials can vary greatly. The thermal stability of indoor air temperature corresponds directly with the density of the inner material. Higher density correlates with stronger thermal stability, whereas lower density results in weaker stability.

Table 3: The heat construction factor of different outer insulation- exterior wall

Name of Composite wall	Serial number	R_T m^2.K/W	C kJ/kg.K	φ_{ii}	φ_{ie}	φ_{ee}
EPS external insulation wall	1	2.8826	526.16	0.5898	0.1486	0.0689
EPS internal insulation wall	2	2.8839	528.88	0.0698	0.0724	0.7896
EPS central wall	3	2.8889	528.84	0.3898	0.0898	0.4458
EPS central wall1	4	2.8868	554.44	0.1898	0.2488	0.2868
Cast-in-place reinforced concrete polystyrene board external insulation wall	5	2.7588	758.44	0.7148	0.1088	0.0478
Cast-in-place reinforced concrete polystyrene board internal insulation wall	6	2.7598	758.48	0.0469	0.0588	0.8688
Cast-in-place reinforced concrete polystyrene board central wall	7	2.7688	768.48	0.4128	0.0588	0.5488
Cast-in-place reinforced concrete polystyrene board central wall1	8	2.7588	758.48	0.2168	0.2544	0.2798

3.2 Heat balance analysis of the building envelope using the Energy Plus mathematical model

The mathematical model of wall heat transfer is the basis of the Energy Plus calculation. As the part of the wall in closest contact with the outside environment, the correct calculation of the transient heat transfer of the wall thermal system under any disturbance is the key to calculating the energy consumption of the building. To analyse the dynamic thermal characteristics of the building envelope, especially under transient conditions, the thermal response factor method is generally used for calculation. The thermal response factor method is the basis for calculating the cooling and heating loads of air conditioning systems and for analysing the annual energy consumption of buildings. The calculation principle is to calculate the response of the internal and external surface temperature and heat flow of the envelope to the unit delta wave temperature disturbance [13], and to calculate the heat absorption, heat release and heat transfer response coefficients of the envelope. Then the arbitrary change of outdoor temperature is decomposed into an iterable delta wave, which can be iterated by using the differential equation of thermal conductivity. The temperature and heat flow of the box surface at any given time are obtained by iterating the response of the box to each temperature delta wave.

The integrated outside air temperature over time is

Tout (τ)The change in the internal air temperature between Tin (τ),then the heat conducted through the internal surface of the enclosure at time n is

$$q_{in}(n) = \sum_{j=0}^{\infty} Y(j)T_{out}(n-j) - \sum_{j=0}^{\infty} Z(j)T_{in}(n-j) \quad (36)$$

The heat conducted through the external surface of the envelope at moment n is

ISSN 2663-1563 Vol. 6, Issue 1: 26-41, DOI: 10.25236/AJAGE.2024.060105

$$q_{out}(n) = \sum_{j=0}^{\infty} X(j)T_{out}(n-j) - \sum_{j=0}^{\infty} Y(j)T_{in}(n-j) \quad (37)$$

in the formula :

$Y(j)$ — heat transfer reaction coefficient of the wall.

X (j) — the heat absorption reaction coefficient of the outer surface of the wall.

$Z(j)$ — the heat absorption reaction coefficient of the internal surface of the wall

Due to the rapid decay of the reaction coefficient, Energy Plus uses the thermal conductivity transfer function method instead of the reaction coefficient method in the traditional sense, and the basic equation is as follows

The heat transferred through the inner surface of the envelope at time n is

$$q_{in}(n) = \sum_{j=0}^{nz} Y(j)T_{out}(n-j) - \sum_{j=0}^{nz} Z(j)T_{in}(n-j) \quad (38)$$

The heat conducted through the external surface of the envelope at moment n is

$$q_{out}(n) = \sum_{j=0}^{nz} X(j)T_{out}(n-j) - \sum_{j=0}^{nz} Y(j)T_{in}(n-j) \quad (39)$$

In this heat transfer problem with a single-layer slab wall, the nodal temperature serves as the state variable, while the input variable is the ambient temperature (both inner and outer surfaces). In this heat transfer problem with a single-layer slab wall, the nodal temperature serves as the state variable, while the input variable is the ambient temperature (both inner and outer surfaces). The output result is the heat flux at various surfaces. In this heat transfer problem with a single-layer slab wall, the nodal temperature serves as the state variable, while the input variable is the ambient temperature (both inner and outer surfaces). We now present the method for creating the state node equations as an illustrative example. As demonstrated in Figure 4, a flat wall possessing a known surface area A and thickness L features a convective heat transfer coefficient h on both sides, while the material's thermal and temperature conductivity constants are represented by λ and α, respectively.

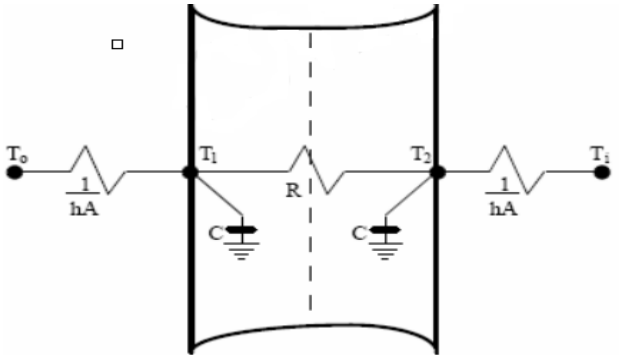

Figure 4: The heat transfer grid of one dimension slab

Node 1:

$$C\frac{dT_1}{d\tau} = hA(T_o - T_1) + \frac{T_2 - T_1}{R} \quad (40)$$

Node 2:

$$C\frac{dT_2}{d\tau} = hA(T_i - T_2) + \frac{T_1 - T_2}{R} \quad (41)$$

In the glass window model, heat is transferred into the room through the window glass due to the combined effect of solar radiation and the difference between the indoor and outdoor temperatures. After the sunlight hits the surface of the window glass, some of it is reflected and all of it does not become the heat gain of the room; some of the solar radiation energy passes through the glass directly into the room in the form of short-wave radiation and all of it becomes the heat gain of the room, which is mainly determined by the solar radiation and the optical properties of the glass; and the glass absorbs another part of the solar radiation energy and raises its own temperature, and then dissipates heat to the room in the form of convection and long-wave radiation. Convection and long wave radiation dissipate heat into the room and outside [14]. The heat balance equation for the glass surface in Energy Plus is mainly based on the following assumptions.

(1) The thickness of the glass is so thin that the change in its heat capacity can be ignored.

ISSN 2663-1563 Vol. 6, Issue 1: 26-41, DOI: 10.25236/AJAGE.2024.060105

(2) The direction of heat flow is perpendicular to the glass surface and is one-dimensional.

(3) The glass surface is opaque to long wave radiation.

(4) The inner and outer surfaces of the glass are isothermal.

(5) The short-wave radiation absorbed by the glass is distributed in the same proportion to the inner and outer surfaces.

Figure 5 shows a double glazing system with the following heat balance equation for the four surfaces: Single layer

The heat balance equation for glass or multilayer glass is similar.

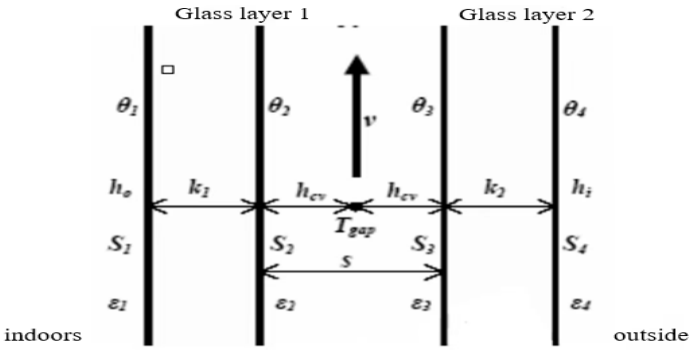

Figure 5: Heat balance diagram of double glazing system

Changes in the intensity of the point heat source qs resulting from fluctuations in the indoor and outdoor surroundings or the instability of the energy source can be viewed as a sequence of step signals at intervals of time.

$$\theta^{(r+1)} = \sum_{j=0}^{N}\left\{\frac{q_s^{(r-j)}-q_s^{r-j-1}}{4\pi\gamma}\sum_{i=0}^{m}\int_0^{j\Delta h}\frac{1}{t}exp(-\frac{r_i^2}{4at}-\omega^2 at)dt\right\} \quad (42)$$

The time series is shown in Figure 6:

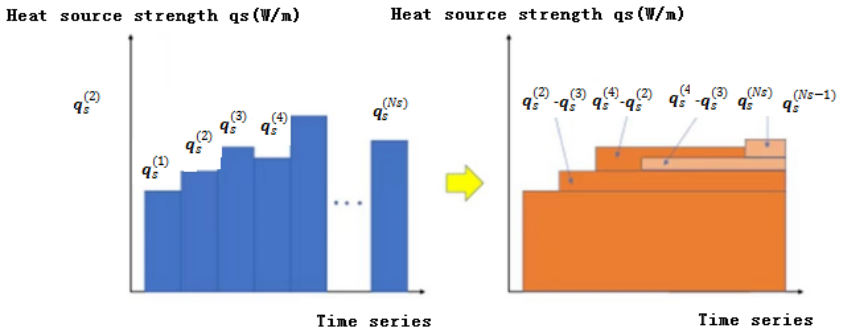

Figure 6: Schematic diagram of the transformation of the dynamic changes of the point heat source

At the model parameters Tin = 24.1 °C, Ti = 36.1 °C, I = 1.21 A, δ = 0.002 m, qs = 230.1 W/m K, and a default size of 0.315 m × 0.406 m for a typical region, the curvilinear relationships for radiant panels of different thicknesses are shown in Figure 7.

ISSN 2663-1563 Vol. 6, Issue 1: 26-41, DOI: 10.25236/AJAGE.2024.060105

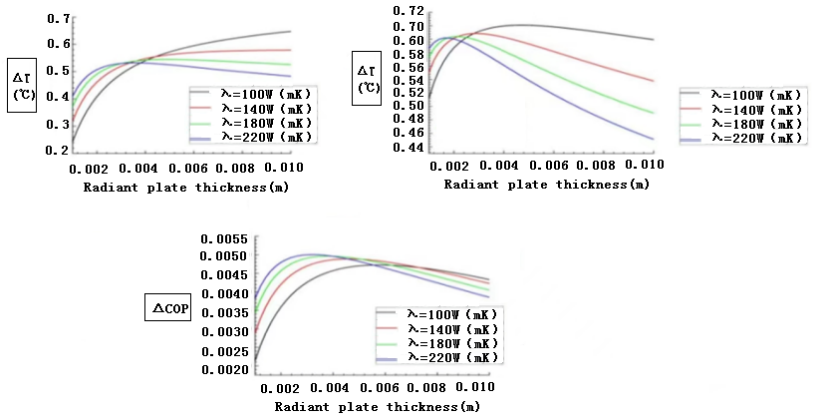

Figure 7: The influence curve of radiation plate thickness on the temperature field

The impact of thermal conductivity on the temperature field is more noticeable within a specific range and when thermal conductivity is low. This highlights the importance of the temperature gradient along the thickness direction of the radiant plate in the simulation of the overall temperature field [15]. Figure 8 illustrates the curve outlining the influence of the area factor on the heat balance of the structure being maintained.

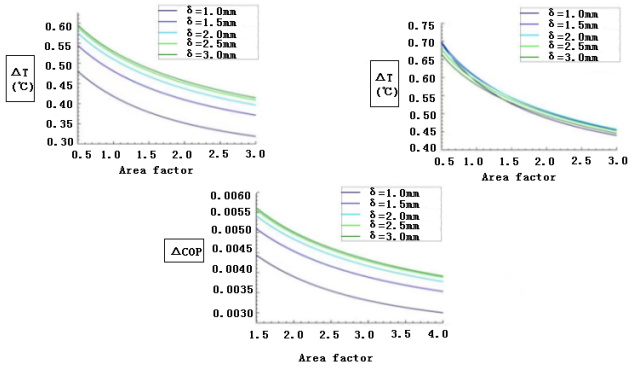

Figure 8: Curve of the effect of area factor on the temperature field

The thermal conductance impact curve on the heat equilibrium of the upkeep framework is displayed in Figure 9.

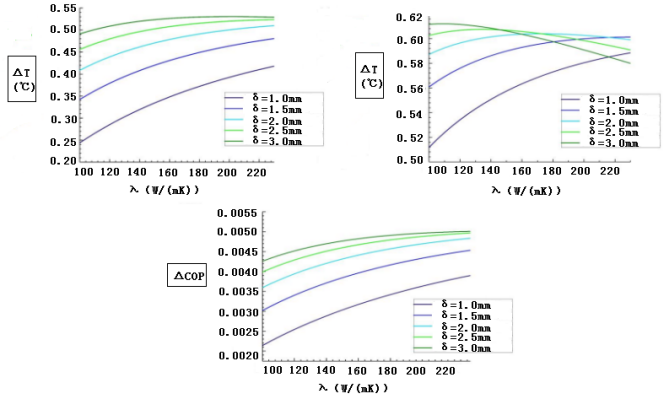

Figure 9: Curve of thermal conductivity on temperature field

For an internal insulation composite wall of identical properties, the thermal resistance increases and the heat capacity of the indoor-facing material decreases as the wall ϕii decreases. This results in a smaller amount of heat change that is stored in the wall due to changes in ambient temperature. The lower the proportion of heat change retained within the wall, the less heat exchanged between the wall and indoor air, leading to reduced stability of indoor temperature [16, 17]. The effect of composite walls on ambient temperature change is linked to the heat capacity of the envelope material, which rises with increases in

ISSN 2663-1563 Vol. 6, Issue 1: 26-41, DOI: 10.25236/AJAGE.2024.060105

material density, specific heat, and thickness. In terms of building walls, there is relatively little difference in the specific heat and thickness of various materials. However, the density of different materials varies greatly. It is worth noting that the higher the density of the inner material, the greater the thermal stability of indoor air temperature. Conversely, the lower the density of the inner material, the weaker the thermal stability of indoor air temperature. The thermal stability of indoor air temperature is improved and the ϕii of external insulation composite wall 1 is greater than that of wall 5. The simulation results reveal that composite walls 1 and 3 possess smaller average heating energy consumption indexes than composite walls 2 and 4, respectively. On the other hand, composite walls 5 and 7 have larger average heating energy consumption indexes than composite walls 6 and 8, respectively. The discrepancy can be attributed to the fact that composite walls 1 and 3 possess greater ϕii values than composite walls 2 and 4, respectively, and that composite walls 5 and 7 exhibit greater ϕ than composite walls.

The small ϕii values of bodies 6 and 8 are clarified. Composite wall buildings with a low thermal structure factor ϕii have a considerable heat capacity and a minimal thermal resistance on the interior wall side. The temperature alterations result in a lesser proportion of variation in the heat trapped in the wall on account of a shift in ambient temperature. For both types of externally insulated and internally insulated walls, the thermal structure's internal factor ϕii is greater for externally insulated walls as opposed to internally insulated walls. Therefore, for an energy-efficient building wall, it is recommended to arrange the load-bearing structural part with high heat capacity on the interior side and the insulation with high thermal resistance on the exterior side. This helps to mitigate the impact of indoor and outdoor temperature changes on the room temperature and minimize heating energy consumption.

4. Conclusions

The paper presents the application of the similitude theory in studying the unsteady heat conduction of composite walls. A theoretical method is developed and its correctness is verified through an example. The thermal structure factor is then introduced to analyze the thermal properties of composite walls. This factor reflects the arrangement order of materials within the wall and is dependent on heat capacity and thermal resistance along the thickness direction. The paper proposes the application of similarity theory to obtain the analytical solution of the temperature field related to the unsteady heat conduction in composite walls. Additionally, the Green function is introduced to improve the interpretation of the unsteady heat conduction in composite walls. The thermal structure factor is defined as a function of the heat capacity and thermal resistance along the thickness direction of the composite wall. Further research is required to thoroughly explore the analytical solution of unsteady heat conduction in composite walls. The study further investigates the analytical solution for unsteady heat conduction in a composite wall under real weather conditions. Additionally, it explores the application of the Green function method to analyse wall energy consumption. On-site testing of actual energy-saving buildings can be conducted throughout the year, allowing for simultaneous evaluation of buildings with distinct characteristics.

5. Discussion

This paper examines the impact of various structural factors on thermal energy consumption of composite walls and building envelopes by analyzing their thermal characteristics and simulating energy consumption through Energy Plus software. Our hypothesis is verified through this analysis. The paper's innovation lies in the introduction of similarity theory. An analytical solution for the unsteady heat conduction temperature field of composite walls is presented along with the proposal of a thermal structure factor to reflect the ordering of materials in each layer of the composite wall. Objective language is used throughout, technical term abbreviations are explained upon first usage, and clear causal connections are established between statements. The paper's structure follows conventional academic standards and employs precise word choice. The text is free of grammatical errors, punctuation mistakes and spelling errors. Currently, the analytical solution for unsteady heat conduction in composite walls requires further research depth, especially concerning real meteorological conditions. Moreover, supporting theoretical research is still necessary to establish the feasibility of software modification based on experimental data. The simplified calculation model for envelope loading presented in this paper enables the efficient and precise estimation of the cooling and heating load index and the annual cumulative cooling and heating load of the envelope structure following the determination of basic thermodynamic parameters. This model holds immense value and relevance for promoting energy conservation and facilitating sustainable development. The present all-inclusive load calculation model has been designed to anticipate the cold and heat load index of building envelopes and the yearly amassed cold and heat load in an objective manner. This facilitates the full utilization of rapid and precise envelope

ISSN 2663-1563 Vol. 6, Issue 1: 26-41, DOI: 10.25236/AJAGE.2024.060105

load calculations, which can further be validated through engineering practices. Through the use of existing building object simulation calculations, the all-encompassing load calculation model of other cities can also be obtained.

Acknowledgement

This work was supported by Research platform of Study on the spatial characteristics of traditional mountainous rural settlements in Hechuan area of Chongqing from the perspective of rural revitalization (22CRKPT0201), Foundation project of Research on School-level project: "Energy-saving design and application of green public building energy system in Chongqing "(Project No. CRKZK2022003), the Faculty-level project "Regionalized bridge structure health management based on big data technology" (Project No. CRKGS202103K) and Prediction Study on Achieving the Strategic Goal of "Carbon Neutral, Carbon Peak" in Chongqing (Municipal Project, 22SKGH500).Study on the maturity evaluation of BIM application capability in construction projects based on tomographic analysis method (020101).

References

[1] Jun L. 2005. Building Energy Ratio and Building Energy Efficiency Targets. China Energy. 27(10): 23–27.
[2] Zhang G. 1998. Model of dynamic thermal properties of building envelope and its identification. Journal of Hunan University. 25(3): 67–71.
[3] Chen Y, Zhou J, Peng J. 2004. Research on the development of dynamic thermal property data sheets for commonly used walls and roofs. Building Thermal Ventilation and Air Conditioning. 23(2): 18–21.
[4] Sun D. Higher Heat Transfer. China Construction Industry Press. 2005: 57-65.
[5] Hu H. 1998. Generalized Green's functions and Green's function solutions for heat conduction problems. Journal of the University of Science and Technology of China. 28(6): 718–721.
[6] McMasters RL, Dowding KJ, Beck JV, Yen DHY. 2002. Methodology to generate accurate solutions for verification in transient three-dimensional heat conduction. Numer Heat Tr B-Fund. 41(6): 521–541. doi:https://doi.org/10.1080/10407790190053761.
[7] Norford LK, Socolow RH, Hsieh ES, Spadaro GV. 1994. Two-to-one discrepancy between measured and predicted performance of a "low-energy" office building: insights from a reconciliation based on the DOE-2 model. Energ Buildings. 21(2):121–131. doi:https://doi.org/10.1016/0378-7788 (94)90005-1.
[8] Reddy TA, Claridge DE. 1994. Using synthetic data to evaluate multiple regression and principal component analyses for statistical modeling of daily building energy consumption. Energ Buildings. 21(1):35–44. doi:https://doi.org/10.1016/0378-7788 (94)90014-0.
[9] Luo Y, Zhang L, Liu Z, Wu J, Wang X, Xie L, et al. 2017. Building Integrated Photovoltaic Thermoelectric Wall System: Balancing Simulation Speed and Accuracy. Energy Procedia. 105:88–93. doi:https://doi.org/10.1016/j.egypro.2017.03.284.
[10] Khire RA, Messac A, Van Dessel S. 2005. Design of thermoelectric heat pump unit for active building envelope systems. Int J Heat Mass Tran. 48(19-20):4028–4040. doi: https://doi.org/10. 1016/j. ijheatmasstransfer.2005.04.028.
[11] Van Dessel S, Foubert B. 2010. Active thermal insulators: Finite elements modeling and parametric study of thermoelectric modules integrated into a double pane glazing system. Energ Buildings. 42(7):1156–1164. doi:https://doi.org/10.1016/j.enbuild. 2010.02.007.
[12] Sirisha Rangavajhala, Ritesh Khire, Achille Messac. 2006 Sep 6. Impact of Weather Uncertainties on Active Building Envelopes (ABE): An Emerging Thermal Control Technology. 11th Multidisciplinary Analysis and Optimization Conference, Portsmouth, Virginia, September. doi: https://doi.org/ 10.2514/6. 2006-7093.
[13] Witte MJ, Henninger RH, Glazer J, Crawley DB. 2001 Jan 1. Testing and validation of a new building energy simulation program. Proceedings of Building Simulation, Brazil. 353–360. https://www.aivc.org/resource/testing-and-validation-new-building-energy-simulation-program.
[14] Chan DSH, Padang JCH. 1987. Analytical methods for the extraction of solar-cell single- and double-diode model parameters from I-V characteristics. In IEEE T Electron Dev, 34(2): 286-293. doi: 10.1109/T-ED. 1987.22920.
[15] Tuhus-Dubrow D, Krarti M. 2010. Genetic-algorithm based approach to optimize building envelope design for residential buildings. Build Environ. 45(7):1574–1581. doi:https://doi.org/ 10.1016/j. buildenv. 2010.01.005.
[16] Delisle V, Kummert M. 2014. A novel approach to compare building-integrated

ISSN 2663-1563 Vol. 6, Issue 1: 26-41, DOI: 10.25236/AJAGE.2024.060105

photovoltaics/thermal air collectors to side-by-side PV modules and solar thermal collectors. Sol Energy. 100:50–65. doi: https://doi.org/10.1016/j.solener. 2013.09.040.
[17] Yu J, Tian L, Xu X, Wang J. 2015. Evaluation on energy and thermal performance for office building envelope in different climate zones of China. Energ Buildings. 86:626–639. doi:https://doi.org/ 10.1016/j. enbuild.2014.10.057.